WATER RESOURCES RESEARCH, VOL. 34, NO. 4, PAGES 623–636, APRIL 1998

Effect of enhanced manganese oxidation in the hyporheic zone on basin-scale geochemical mass balance

Judson W. Harvey
Water Resources Division, U.S. Geological Survey, Reston, Virginia

Christopher C. Fuller
Water Resources Division, U.S. Geological Survey, Menlo Park, California

Abstract. We determined the role of the hyporheic zone (the subsurface zone where stream water and shallow groundwater mix) in enhancing microbially mediated oxidation of dissolved manganese (to form manganese precipitates) in a drainage basin contaminated by copper mining. The fate of manganese is of overall importance to water quality in Pinal Creek Basin, Arizona, because manganese reactions affect the transport of trace metals. The basin-scale role of the hyporheic zone is difficult to quantify because stream-tracer studies do not always reliably characterize the cumulative effects of the hyporheic zone. This study determined cumulative effects of hyporheic reactions in Pinal Creek basin by characterizing manganese uptake at several spatial scales (stream-reach scale, hyporheic-flow-path scale, and sediment-grain scale). At the stream-reach scale a one-dimensional stream-transport model (including storage zones to represent hyporheic flow paths) was used to determine a reach-averaged time constant for manganese uptake in hyporheic zones, $1/\lambda_s$, of 1.3 hours, which was somewhat faster but still similar to manganese uptake time constants that were measured directly in centimeter-scale hyporheic flow paths ($1/\lambda_h$ = 2.6 hours), and in laboratory batch experiments using streambed sediment ($1/\lambda$ = 2.7 hours). The modeled depths of subsurface storage zones (d_s = 4–17 cm) and modeled residence times of water in storage zones (t_s = 3–12 min) were both consistent with direct measurements in hyporheic flow paths (d_h = 0–15 cm, and t_h = 1–25 min). There was also good agreement between reach-scale modeling and direct measurements of the percentage removal of dissolved manganese in hyporheic flow paths (f_s = 8.9%, and f_h = 9.3%). Manganese uptake experiments in the laboratory using sediment from Pinal Creek demonstrated (through comparison of poisoned and unpoisoned treatments) that the manganese removal process was enhanced by microbially mediated oxidation. The cumulative effect of hyporheic exchange in Pinal Creek basin was to remove approximately 20% of the dissolved manganese flowing out of the drainage basin. Our results illustrate that the cumulative significance of reactive uptake in the hyporheic zone depends on the balance between chemical reaction rates, hyporheic porewater residence time, and turnover of streamflow through hyporheic flow paths. The similarity between the hyporheic reaction timescale ($1/\lambda_s \approx 1.3$ hours), and the hyporheic porewater residence timescale ($t_s \approx 8$ min) ensured that there was adequate time for the reaction to progress. Furthermore, it was the similarity between the turnover length for stream water flow through hyporheic flow paths (L_s = stream velocity/storage-zone exchange coefficient $\approx$ 1.3 km) and the length of Pinal Creek ($L \approx 7$ km), which ensured that all stream water passed through hyporheic flow paths several times. As a means to generalize our findings to other sites where similar types of hydrologic and chemical information are available, we suggest a cumulative significance index for hyporheic reactions, $R_s = \lambda_s t_s L/L_s$ (dimensionless); higher values indicate a greater potential for hyporheic reactions to influence geochemical mass balance. Our experience in Pinal Creek basin suggests that values of $R_s > 0.2$ characterize systems where hyporheic reactions are likely to influence geochemical mass balance at the drainage-basin scale.

1. Introduction

1.1. Role of Hyporheic Zone in Reactive Solute Transport

Channel water in rivers and streams is diverted through subsurface (hyporheic) flow paths and mixed with groundwater in close contact with geochemically and microbially active sediment surfaces. The resulting prolonged contact of channel water with sediment appears to be responsible for enhancing solute reactions in drainage basins. A key process is the advection of dissolved oxygen into the hyporheic zone, which stimulates the activity of aerobic microorganisms on hyporheic-zone sediments when dissolved organic carbon is readily available [*Findlay et al.*, 1993; *Rutherford et al.*, 1995; *McMahon*

Paper number 97WR03606.

et al., 1995]. High microbial activity in the hyporheic zone affects nitrogen cycling by stimulating nitrification and denitrification reactions [*Triska et al*., 1993]. Other important chemical reactions also appear to be enhanced in the hyporheic zone, including sorption of dissolved metals to sediments [*Bencala et al*., 1984; *Cerling et al*., 1990], uptake of phosphorus [*Mulholland et al*., 1997], oxidation of dissolved metals to form metal precipitate coatings on sediment [*Kimball et al*., 1994; *Benner et al*., 1995], and biodegradation of organic contaminants such as toluene [*Heekyung et al*., 1995].

Manganese often is not the most toxic metal at mining sites, but that understates its importance because the fate of manganese in the environment affects the transport of other trace metals. For example, at Pinal Creek, trace metals such as cobalt (600 μg L^{-1}), nickel (1200 μg L^{-1}), and zinc (600 μg L^{-1}) are affected by the fate of manganese because they coprecipitate with manganese oxides [*Hem*, 1981]. Also, several studies in Europe determined complex interactions between nutrients, organic carbon, trace metals, and manganese dissolution (followed by oxidation) in shallow groundwater that affect drinking water quality. Those interactions occur when contaminated river water infiltrates alluvial aquifers in response to pumping at water supply wells [*von Gunten and Lienert*, 1993; *Bourg and Bertin*, 1993]. Enhanced uptake of dissolved manganese in hyporheic zones very likely occurs in hyporheic zones of other U.S. streams, such as in the coal mining areas of the Appalachian Mountains of the eastern United States, where streams often have near-neutral *p*H and manganese concentrations are often between 10 and 200 mg L^{-1} [*Tarutis et al*., 1992; D. White, personal communication, 1997].

1.2. Investigating the Cumulative Effects of Hyporheic Processes

Relatively few studies have quantified reach-scale effects of hyporheic reactions, and researchers have begun to question whether enhanced chemical reactions in the hyporheic zone are important at the drainage-basin scale [*Findlay*, 1995]. The problem in quantifying basin-scale effects of hyporheic reactions is due in part to the disparity of scales between small-scale (1–10 cm) hyporheic processes and large-(basin)-scale effects. Small-scale investigations are essential to identify processes, yet results are usually too variable from site to site to reliably quantify cumulative effects. On the other hand, stream-tracer studies (50–500 m) cannot always reliably isolate or distinguish hyporheic-zone processes from other processes [*Harvey et al*., 1996]. A number of previous investigators characterized reactive solute transport by injecting reactive constituents into both the stream and subsurface [*Bencala et al*., 1984; *Triska et al*., 1993; *Valett et al*., 1996]. That strategy is an excellent means to investigate processes; however, because of the substantially elevated concentrations of the reactive constituent, the results might not represent natural reaction rates.

As an alternative to injecting a reactive constituent to determine natural reaction rates, we conducted stream-tracer studies that did not alter natural levels of the reactive constituent in our system. This approach follows the approach used by *Kimball et al*. [1994] and *Heekyung et al*. [1995]. In addition, we independently estimated hyporheic reactions at finer scales (within hyporheic flow paths and in the laboratory) for comparison with the results from our stream-tracer studies. As a result, we were able to quantify the effects of the hyporheic zone on solute mass balance at the drainage-basin scale. To our knowledge this is the first study to quantify reach-scale removal of a solute in the hyporheic zone on the basis of three spatial scales of inquiry.

We hypothesized that if the chemical reaction rate and hydrologic flushing time of the hyporheic zone were similar and if rates were fast enough that all stream water was routed through hyporheic flow paths several times, then the drainage basin mass balance would be significantly affected by the lowering of dissolved manganese concentrations in stream outflow. We tested our idea in Pinal Creek basin through an investigation of enhanced oxidation of dissolved manganese to form manganese oxide precipitates in the hyporheic zone (Figure 1). The input of streamwater to the hyporheic zone enhanced the reaction by increasing the contact of stream water with sediment and microbes, i.e., the reaction catalysts. In addition, the input of streamflow raised the *p*H and the dissolved oxygen concentrations in the hyporheic zone, which further stimulated the rate of manganese oxidation. The cumulative effect of enhanced manganese oxidation in the hyporheic zone was a 20% decrease in the load of manganese flowing out of the drainage basin. We concluded our study by attempting to generalize our findings. To do this, we developed a dimensionless index that uses basic hydrologic and chemical information to quantify the potential for hyporheic reactions to influence solute mass balance at the drainage-basin scale.

2. Study Site

2.1. Hydrogeologic Setting

Pinal Creek basin is located in the central highlands of Arizona in the copper mining district near Globe (Gila County); elevation in the basin ranges from 7800 feet (2378 m) in the Pinal Mountains to 2700 feet (823 m) at the basin outlet. The area of the basin is 516 km^2 of which 170 km^2 is a regional aquifer composed of partially cemented basin fill. A less extensive sand and gravel alluvial aquifer (20 km long by 1 km wide by 50 m deep) is present in the central and lower basin. The aquifer is eventually truncated by igneous rock formations at a location called Inspiration Dam (Figure 2a). The alluvial aquifer becomes constricted above the basin outlet, which forces groundwater to the surface. The resulting perennial streamflow increases from a flow of zero at a point near Setka Ranch to a flow of 0.25 m^3 s^{-1} at a point 7 km downstream at Inspiration Dam (Figure 2a).

The 7 km perennial reach in Pinal Creek is a sand- and gravel-bed stream with an average slope of 1%, an average width of 2.3 m, and an average depth of 15 cm. Pools are almost nonexistent and riffles or cascades are fairly unusual. The most significant roughness units are cobbles and channel parallel bars at the sides of channels or in the center of channels. Channel-parallel islands as well as fallen tree obstructions, are also present in some areas. Below Inspiration Dam, Pinal Creek enters a rock-walled canyon and flows 6 km to the Salt River (Figure 2b). The Salt River then flows west and empties into Roosevelt Lake, a major water supply reservoir for the City of Phoenix.

2.2. Historic and Present Contamination

A major contributor to contamination at Pinal Creek basin was the release of waste solutions from the leaching of copper ore with sulfuric acid. In approximately 50 years the highly acidic leading edge of the contaminant plume ($p\mathrm{H} \approx 4$) moved 15 km down gradient through the alluvial aquifer beneath the

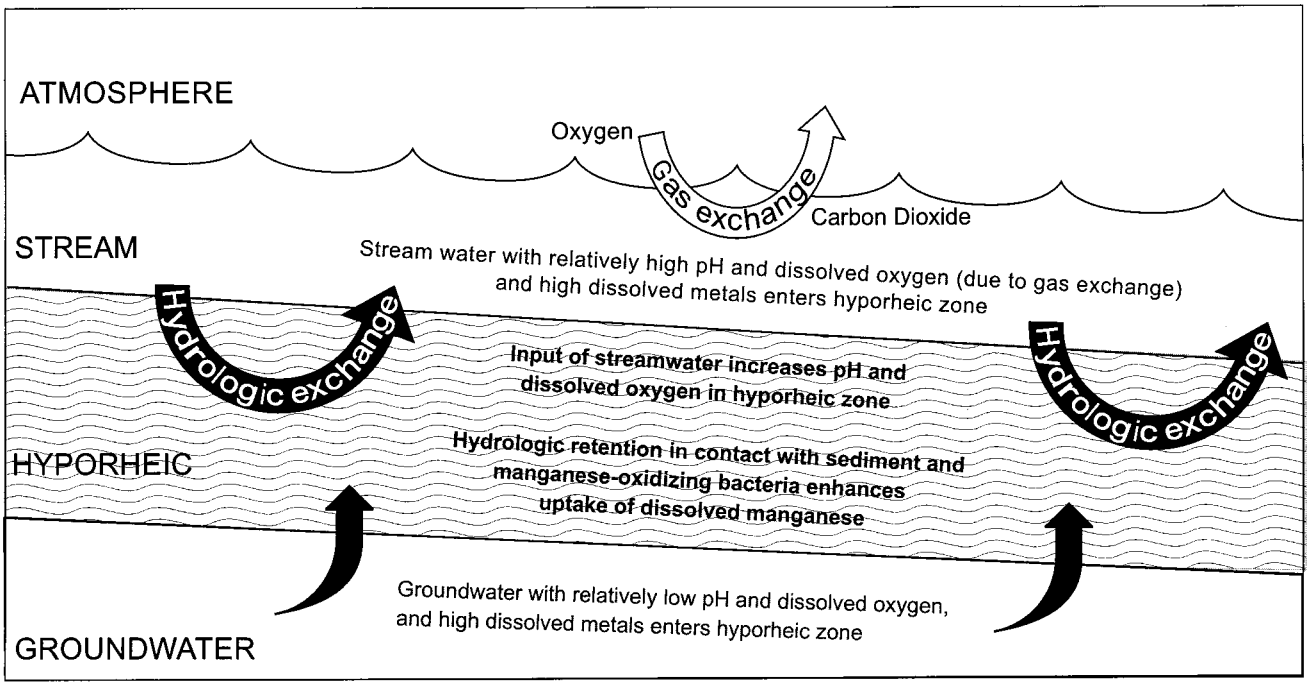

Figure 1. Schematic diagram illustrating factors that enhance oxidation of manganese to form oxide coatings on sediments of the hyporheic zone.

ephemeral streambed into lower Pinal Creek basin (Figure 2). At the leading edge of the acidic plume the movement of dissolved metals was retarded by neutralization reactions with carbonate and silicate minerals that exist naturally in the basin [*Stollenwerk*, 1994]. Wherever neutralization occurred, dissolved iron oxidized to form precipitates and manganese dissolved, releasing high concentrations of manganese into groundwater [*Glynn and Brown*, 1996]. As a result, a neutralized groundwater plume contaminated with manganese moved ahead of the acidic plume and, beginning in ~1979, began discharging into the perennial reach of Pinal Creek.

The perennial portion of Pinal Creek extends 7 km, from the head of perennial flow 1.5 km upstream of Setka Ranch to the outlet of Pinal Creek basin at Inspiration Dam (Figure 2). Most of the groundwater discharge to Pinal Creek occurs in the first 2 km downstream of the head of perennial flow (Figure 2a). The location where groundwater discharge to Pinal Creek is greatest is also the point where groundwater is most contaminated. Currently that part of the plume has a *p*H of ~5.5, low dissolved oxygen (~0.1 mg L^{-1}), high-dissolved solids (SO_4 2,200 mg L^{-1}; Ca 500 mg L^{-1}), elevated pCO_2 ($10^{-0.94}$) resulting from neutralization reactions, and elevated concentrations of manganese (80 mg L^{-1}), nickel (1200 μg L^{-1}), cobalt (600 μg L^{-1}), and zinc (1200 μg L^{-1}). Smaller amounts of groundwater also discharge to Pinal Creek farther down the valley, but that water is much less contaminated and has the primary effect of diluting dissolved metal concentrations in surface water.

Significant manganese oxidation does not occur in the neutralized contaminated part of the groundwater plume at Pinal Creek basin because of the relatively low *p*H and dissolved oxygen concentrations [*Glynn and Brown*, 1996; *Stollenwerk*, 1994]. Once groundwater enters the stream, both *p*H and dissolved oxygen increase in the downstream direction because of gas exchange (Figure 3). Thermodynamically, the increase in *p*H and dissolved oxygen in streamflow favors the oxidation of dissolved manganese to form manganese oxides [*Davies and Morgan*, 1989]; however, manganese does not readily oxidize in surface water without sediment [*Hem*, 1981]. We confirmed that suspended sediments and colloids in Pinal Creek streamflow were not causing significant oxidation of manganese in Pinal Creek streamflow [*Harvey and Fuller*, 1996]. More likely, oxidation of dissolved manganese was occurring in contact with surface coatings on sediments such as iron oxides or manganese-oxidizing bacteria, each of which potentially has a role in catalyzing the reaction [*Diem and Stumm*, 1984].

3. Methods

3.1. Chemical Sampling

A solute tracer was injected into streamflow in order to characterize reach-scale hydrologic transport parameters. KBr (potassium bromide) was dissolved in stream water in large containers next to the stream and then injected at a constant rate into the stream until concentrations reached plateau concentrations at all sampling sites. We used the experimental design approach recommended by *Wagner and Harvey* [1997] to select sampling distances and determine frequency of sampling as a means of increasing the reliability of hydrologic parameters to be estimated by modeling. Surface water samples were collected by dipping stream water with pitchers from areas where surface flow was concentrated and fast. Porewater samples for chemical analysis were obtained from shallow groundwater (30, 60, 100, and 200 cm) by pumping from 3/8" stainless steel drive points. We tested whether our stainless-steel drivepoints would create problems by releasing metals. To do this we pumped a laboratory-mixed artificial streamwater made without heavy metals through the samplers; no release of dissolved metals was detected.

Porewater samples from shallower depths in the hyporheic

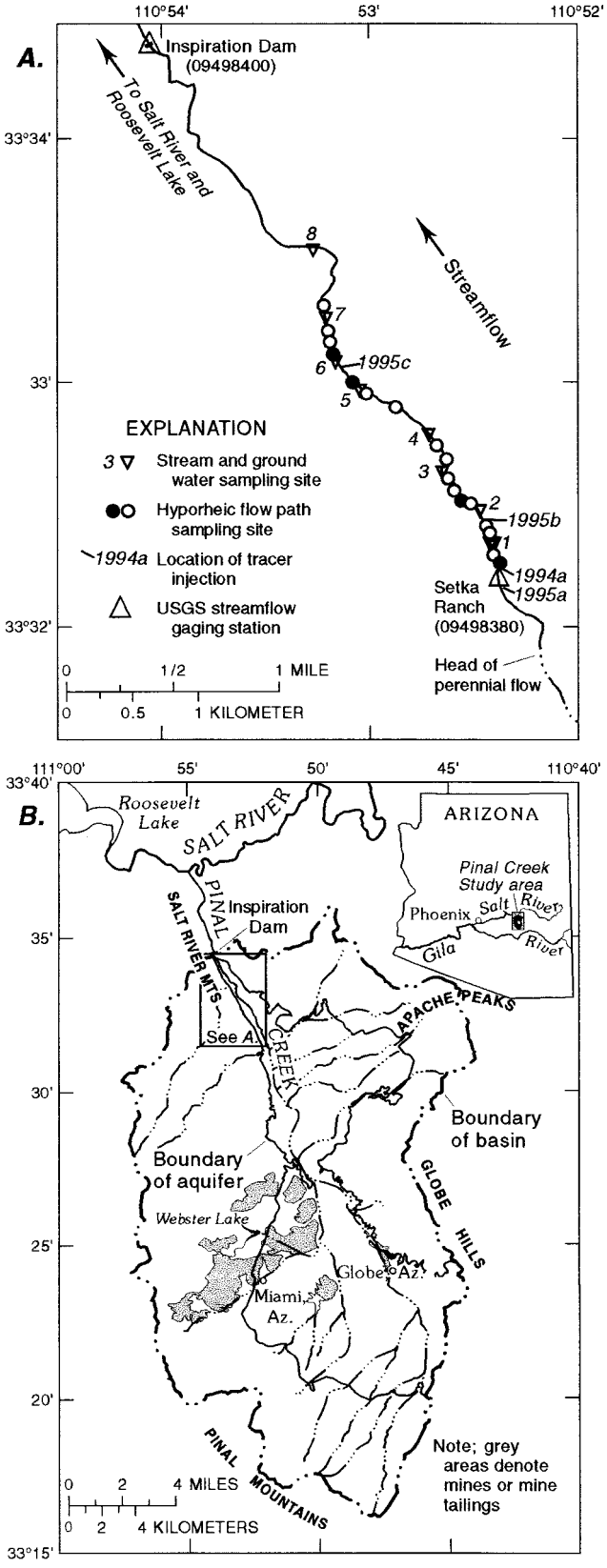

Figure 2. Pinal Creek basin study area: (a) map showing location of stream tracer injections and sampling in 7 km part of Pinal Creek where streamflow is perennial and (b) map showing entire drainage basin with inset map to identify the specific study area where groundwater discharges to the perennial part of Pinal Creek.

zone (2.5 cm vertical intervals) were obtained by peristaltic pumping from small diameter (1/8" od) stainless steel tubes with a 1 cm slot cut near the end. Six tubes were emplaced simultaneously by pushing on a common stem to insert each point to the desired depths (2.5, 5.0, 7.5, 10.0, 12.5, and 15.0 cm). We minimized possible disturbances of the natural patterns of subsurface water flow by pumping very slowly (~5 mL min^{-1}) and by keeping sample volumes small (5–40 mL). The performance of the sampler that we used was recently tested by *Duff et al.* [1998], who found that the sampler did not disturb natural solute gradients in Pinal Creek and in a sand-bed stream similar to Pinal Creek in Minnesota..

Water samples for complete chemical analysis were filtered (0.45 μm) and split between acidified and unacidified bottles for analysis of metals and major cations and anions, respectively; *p*H was measured immediately in the field, and alkalinity samples were collected in glass bottles and transported to a nearby laboratory for analysis within 12 hours. Cations were analyzed by inductively coupled plasma atomic emission spectroscopy (ICP) and anions were measured by ion chromatography (IC). Detection limits were determined by standard procedures, and the reliability of measured concentrations were estimated by computing an average coefficient of variation for a number of replicate determinations. When optimized to detect manganese concentrations that ranged between 10^{-4} and 10^{-3} moles L^{-1}, the ICP had a detection limit of 10^{-6} moles L^{-1} and a reliability of 3%. When optimized to detect bromide concentrations that ranged between 0.2 and 6 mg L^{-1}, the IC had a detection limit of 0.02 mg L^{-1} and a reliability of 2.5%.

3.2. Sediment Characterization

Sediment porosity and the concentration of manganese solid phases in Pinal Creek sediment were determined by coring the streambed to a depth of up to 30 cm at four of the hyporheic flow-path study sites (locations shown by solid circles in Figure 2a). Cores were sectioned into 3 or 4 cm increments, air dried, and then weighed. Sediment porosity was determined for each core section on the basis of the volume of each core section, its weight, and the assumption that sediment particles had a density of 2.7 g cm^{-3}. The average sediment porosity was 0.31 ± 0.01 (standard error) for the core sections removed from depths <10 cm below the streambed.

For the purpose of quantifying manganese coatings on sediment we assumed that sediment particles >1 mm had negli-

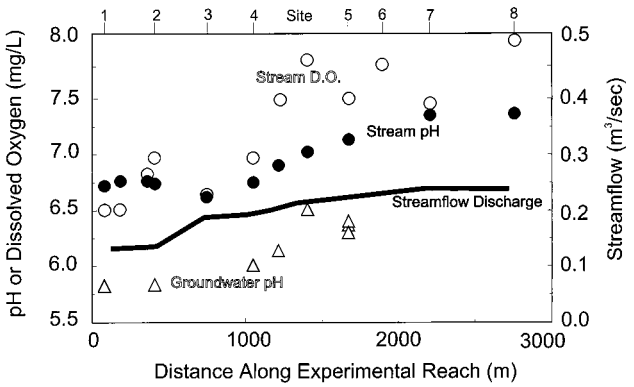

Figure 3. Streamflow discharge and *p*H and dissolved oxygen along the 3 km experimental study reach in Pinal Creek basin. Dissolved oxygen in groundwater is ~0.1 mg L^{-1}.

gible surface area compared to smaller particles. Particles >1 mm were removed from the core samples by dry sieving (the average percent weight of grains <1 mm was 43% ± 2 (standard error). Manganese solid-phase concentrations were determined on splits from the <1 mm fraction from core sections removed from depths <10 cm below the streambed. Metals were extracted from the remaining sediment with 0.1M hydroxylamine hydrochloride in 0.05N HNO_3 (HA) for 1 hour at room temperature on an end-over-end rotator. Extraction under these conditions has been found to be effective in dissolving manganese oxyhydroxide coatings on sediment grains [*Chao*, 1984]. Extract solutions were analyzed by inductively coupled plasma atomic emission spectroscopy. No measurable change in manganese extraction from these sediments was observed when extraction times were lengthened (up to 24 hours) or when a stronger extractant was used at higher temperature (0.25M HA at 50°C). Concentrations of extracted manganese on duplicate splits of each core sample agreed to within 12% or better.

3.3. Laboratory Determination of the Rate of Manganese Oxidation by Streambed Sediments

Laboratory experiments were conducted using Pinal Creek sediment to determine the overall rate of dissolved manganese uptake for comparison to estimates from field data. Sediments were collected from three sites, i.e., from sampling site 5 and from a site near Inspiration Dam (Figure 2a). All sediment was collected from the upper 2 cm of the streambed in areas devoid of benthic algae, sieved to remove particles >1 mm in diameter, and stored wet in containers open to the atmosphere at 4°C in the dark. The time of storage (tested up to 1 year) had no effect on the results.

Uptake of dissolved manganese as a function of time was determined in batch systems (50 mL polycarbonate centrifuge tubes, with a pair of tubes sacrificed at each time point). The aqueous phase used in experiments consisted of a mixture of groundwater obtained from a well located a short distance up the valley from the head of perennial flow in Pinal Creek and an artificial stream water with similar major ion chemistry to Pinal Creek. Experimental *p*H was controlled at 7 ± 0.1 units by fixing the partial pressure of CO_2 with a 1% CO_2 in air mixture. Uptake experiments were initiated by the addition of filtered groundwater preequilibrated with the 1% CO_2-air mixture to the sediment-artificial groundwater mixture to achieve a dissolved manganese concentration similar to stream water. At each time interval, *p*H was measured in a pair of tubes, and supernatant removed for analysis by ICP-atomic emission spectrometry (AES) following centrifugation at 16,000 G for 10 min. Total uptake was calculated from the difference between initial and final manganese concentration. Calculated uptake in duplicate samples agreed to within 3%.

The role of bacteria in manganese oxidation was tested with sediment from a replicate sample at site 5. We used a mixture of sodium azide (2g L^{-1}), tetracycline (0.1g L^{-1}), and penicillin (0.1g L^{-1}) in an equal volume of ambient stream water to poison a split sample from the sediment. This mixture has been found effective in inhibiting microbial manganese oxidation [*Emerson et al*., 1982].

The total uptake of Mn^{2+} by streambed sediments occurs by both reversible and irreversible processes. Reversible uptake of Mn^{2+} includes uptake by adsorption and cation exchange because these processes should respond rapidly and reversibly to changes in dissolved Mn concentration or solution chemistry. Irreversible uptake is due to oxidation of Mn(II) to +3 or +4 oxidation states, which is catalyzed by oxide surfaces [*Davies and Morgan*, 1989] or by microbial processes [*Moffett and Ho*, 1996]. In the experiments the reversible component of manganese uptake at each time point was determined by isotopic exchange [*Davis et al*., 1987; *Payne and Waite*, 1991]. Isotopic exchange was measured by replacing supernatant with ^{54}Mn-labeled artificial stream water of equal total dissolved manganese concentration and measuring the loss of ^{54}Mn from solution in 0.5 hours. The amount of reversible manganese uptake was calculated by mass balance assuming the reversible component of sorbed manganese had reached isotopic equilibrium. Irreversible uptake was calculated by the difference between total and reversible uptake.

4. Stream Reach-Scale: Analyses and Results

Following each tracer injection into Pinal Creek, the bromide concentration rose rapidly after the first arrival of the tracer-labeled water at sampling sites; the rapid initial rise was followed by a period of slower rise in concentration toward a steady plateau concentration. The time needed to reach plateau concentrations depended on the distance from the injection; however, plateau concentrations were always achieved in 4 hours or less following the start of an injection. Tracer data for each experimental injection were analyzed using the following model equations:

$$\frac{\partial C}{\partial t} = -\frac{Q}{A}\frac{\partial C}{\partial x} + \frac{1}{A}\frac{\partial}{\partial x}\left(AD\frac{\partial C}{\partial x}\right) + \frac{q_L}{A}(C_L - C) + \alpha(C_s - C) \quad (1)$$

$$\frac{\partial C_s}{\partial t} = \alpha\frac{A}{A_s}(C - C_s) \quad (2)$$

where C, C_s, and C_L are bromide concentrations in the stream, storage zones, and groundwater respectively [M L^{-3}]; t and x are time and direction along the stream, respectively; Q is the in-stream volumetric flow rate [L^3 T^{-1}]; q_L is groundwater inflow [L^3 L^{-1} T^{-1}]; D is the longitudinal dispersion coefficient in the stream [L^2 T^{-1}]; A and A_s are the stream and storage-zone cross-sectional areas, respectively [L^2]; and α is the storage-zone exchange coefficient [T^{-1}]. Q and q_L were determined by the dilution gauging method as part of the bromide tracer injection [*Kilpatrick and Cobb*, 1985]. The remaining parameters were determined by modeling using one-dimensional transport with inflow and storage (OTIS-P), an extended version of the U.S. Geological Survey (USGS) numerical code by *Runkel and Broshears* [1991] that solves (1) and (2). Following the work of *Wagner and Gorelick* [1986], OTIS-P uses a nonlinear least squares regression package to objectively select a set of parameters (A, D, α, and A_s) for each experimental subreach that closely matched tracer concentrations in the stream measured at the sites shown in Figure 2a. Transport parameters for each subreach are reported in Table 1.

4.1. Using the Reach-Scale Model to Identify Storage Zone Dimensions and Exchange Timescale

To determine whether modeling of storage zones characterizes subsurface hyporheic zones, the storage zone parameters determined above would eventually need to be compared with direct observations of stream water tracer penetration in the hyporheic zone. To facilitate comparisons, we computed the depth of the storage zone from modeling results by assuming

Table 1. Reach-Scale Transport Parameters for Pinal Creek, Arizona, Determined by Modeling Injections of a Bromide Tracer During June 1994 and June 1995

Year and Injection	Reach Endpoints	Reach Length, m	Q,* $m^3 s^{-1}$	q_L^{in}, $\times 10^{-5} m^2 s^{-1}$	q_L^{out} $\times 10^{-5} m^2 s^{-1}$	A,† m^2	D,† $m^2 s^{-1}$	A_s,† m^2	α,† $\times 10^{-4} s^{-1}$
1994a	1–2	303	0.13	3.7	2.2	0.40	0.7	0.13	17
1994a	2–4	588	0.13	7.7	0.0	0.48	0.5	0.10	1.6
1994a	4–5	572	0.18	5.4	0.0	0.38	2.2	0.02	1.6
1994a	5–8	1140	0.21	1.2	3.0	0.35	0.6	0.04	4.3
1995a	1–2	352	0.12	5.1	2.4	0.13	8.3	0.05	3.8
1995b	2–3	271	0.15	18	4.0	0.26	1	0.03	4.3
1995b	3–4	411	0.18	5.1	4.0	0.34	1	0.01	5.9
1995b	4–5	596	0.21	3.9	0.4	0.33	1	0.03	5.1
1995c	6–7	234	0.21	7.7	3.0	0.27	0.5	0.05	17
1995c	7–8	678	0.23	0.0	3.0	0.37	1.5	0.02	4.2

*Q reported is the streamflow discharge at the upstream end of the reach.

†For parameters estimated by the nonlinear least squares optimization approach in Otis-P an estimate of the uncertainty in the parameter estimate is provided. Here we report the uncertainty as a percentage of the best fit parameter estimate based on calculation of the coefficient of variation of the parameter estimate (standard deviation of estimate divided by best fit estimate). The average uncertainty was 1.4% for A, 30% for D, 40% for α, and 18% for A_s.

that solute storage in the subsurface occurred vertically beneath the channel in streambed sediments. We consider this to be a good assumption in streams like Pinal Creek that are much wider than they are deep and where stream cross-sectional area A is much greater than storage zone cross-sectional area A_s. The estimated reach-averaged depth of the storage zone in sediment is estimated from modeling parameters as

$$d_s = \frac{A_s}{wn} \tag{3}$$

where A_s is the model cross-sectional area of the storage zone in a subreach, w is the average stream width measured in that subreach, and n is the average porosity of the streambed sediment at Pinal Creek (0.3). Using all of the modeling results from 1994 and 1995 (Table 1), the subsurface storage-zone depth averaged 8 cm and ranged between 4 and 17 cm.

The average hydrologic residence time in the storage zone is estimated from modeling parameters as

$$t_s = \frac{A_s}{\alpha A} \tag{4}$$

where α is the model storage-zone exchange coefficient and A_s and A are the model cross-sectional area of the storage zone and the stream, respectively. Storage-zone residence times ranged from 3 to 12 min and averaged 8 min for all experimental reaches modeled in 1994 and 1995 (Table 1).

4.2. Reach-Scale Modeling of the Net Manganese Uptake Rate in the Storage Zone

Measurements of manganese concentrations at surface water sampling points and in shallow groundwater were combined with physical transport data to determine a rate constant describing the net uptake rate of dissolved manganese in the storage zones. The following steady state form of the analysis equations was used:

$$0 = -\frac{Q}{A}\frac{\partial C}{\partial x} + \frac{1}{A}\frac{\partial}{\partial x}\left(AD\frac{\partial C}{\partial x}\right) + \frac{q_L}{A}(C_L - C) + \alpha(C_s - C) \tag{5}$$

$$0 = \alpha\frac{A}{A_s}(C - C_s) - \lambda_s C_s, \tag{6}$$

where C, C_s, and C_L represent measured concentrations of manganese or any other solute in the stream, storage zone, and groundwater, respectively; λ_s is a first-order reaction rate constant describing the uptake of that solute in the storage zone; all other parameters are defined as in (1) and (2). Since A, D, α, and A_s were all previously estimated from modeling bromide transport, only λ_s remained to be determined. In each reach, λ_s, the rate constant for manganese oxidation in the storage zone, was adjusted so that the reach-scale simulations would closely match the measured concentrations of dissolved manganese in the stream (Figure 4). The resulting calibrated values of λ_s ranged between 9.5×10^{-5} and 4.0×10^{-4} s^{-1}.

5. Hyporheic-Flow-Path Scale: Analyses and Results

In 1995 we surveyed the depth of tracer movement into the streambed at 13 locations in the 2.6 km experimental reach (Figure 2a) for the purpose of comparison with modeled subsurface storage-zone depths (equation (3)). At each site, bromide concentrations were measured at 2.5, 5.0, and 10 cm below the sediment surface; measurements were made after tracer concentrations plateaued following the start of an injection. The observed depth of the hyporheic zone was estimated by the deepest sampling point where the tracer concentration indicated an input of stream water of 10% or more (compared to groundwater) [*Triska et al.*, 1993]. Results indicated that the bromide tracer moved from depths in the streambed ≥2.5 cm at most sites (11 of 13 sites, 85%) to depths ≥5 cm at 5 of 13 sites (38%) and to depths equal to or greater than 10 cm at 4 of 13 sites (31%).

The comparison of observed tracer movement into the hyporheic zone with reach-averaged depths determined by modeling showed relatively good correspondence between estimates (Figure 5). As might be expected, observed depths of penetration were more variable than reach-scale modeling results. However, in general, reach-scale modeling estimated a

hyporheic-zone depth that followed measured trends of increasing and decreasing hyporheic-zone depths (Figure 5).

Subsurface transport in the hyporheic zone was determined at four sites (two sites in 1994 and two in 1995; the locations of which are shown by solid circles in Figure 2a) that were located relatively close to points of stream injections. Proximity of hyporheic sampling sites to the location of stream injections ensured that tracer arrival at the sampling site would be as rapid as possible, with only a slight (measurable) delay following the start of a stream injection. We followed a relatively straightforward and commonly used approach to estimate hydrologic residence times in hyporheic flow paths [*Triska et al.*, 1993; *Harvey et al.*, 1996]. The increase in tracer concentration

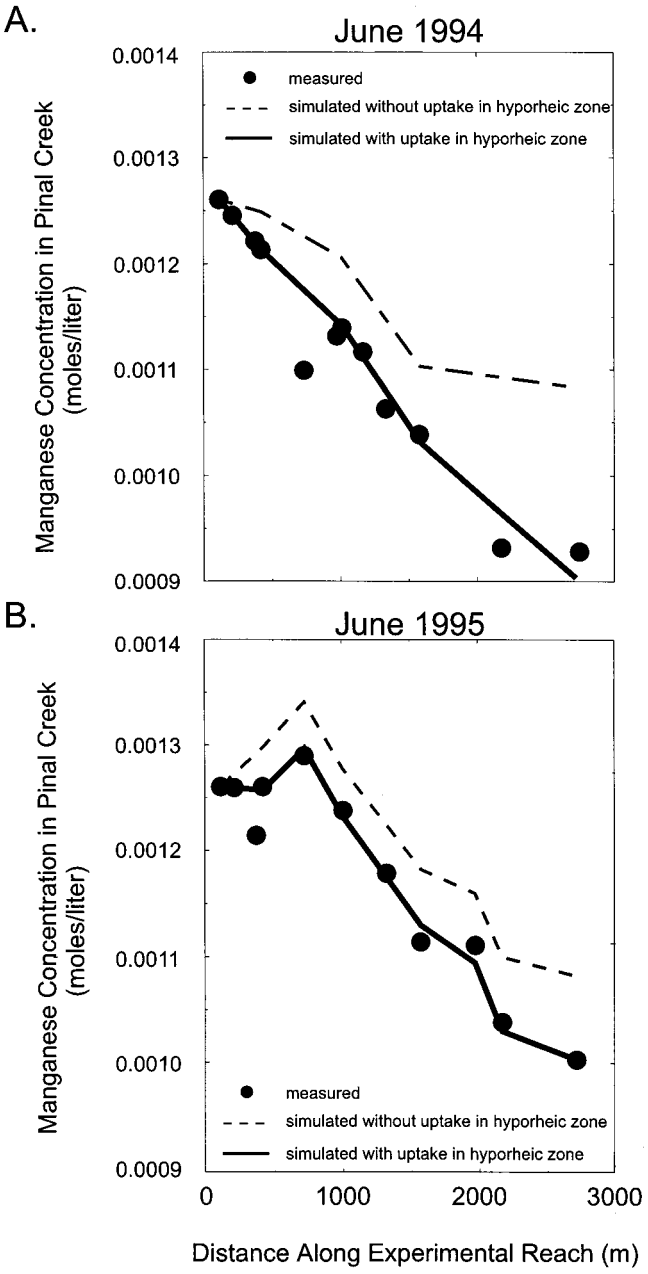

Figure 4. Reach-scale transport simulations for dissolved manganese: (a) June 1994 and (b) June 1995. Alternative simulations indicate the improvement with modeled uptake of dissolved manganese in the hyporheic zone.

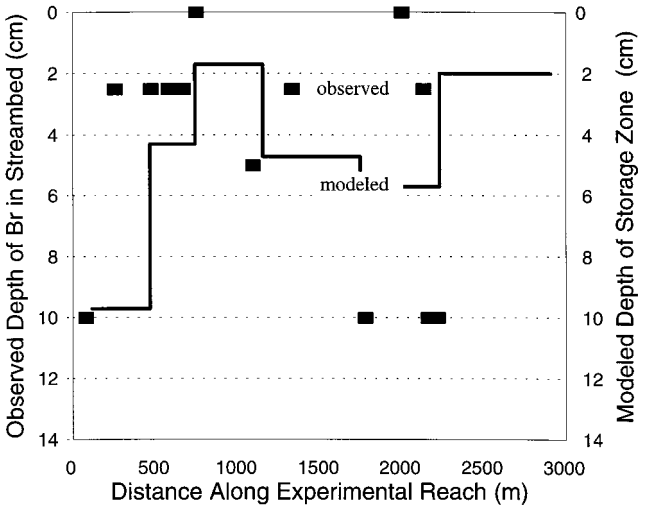

Figure 5. Depth of hyporheic zone determined by modeling stream tracer injections at reach scale compared with direct observations of bromide tracer movement into hyporheic flow paths in the streambed.

was measured as a function of time in surface water and at six depths (2.5, 5.0, 7.5, 10.0, 12.5, and 15 cm) beneath the streambed until plateau concentrations were reached. For each depth that was reached by the bromide tracer the residence time of hyporheic porewater was computed as the elapsed time (since tracer arrival in surface water) for the tracer concentration to reach 1/2 of the eventual plateau concentration. In order to compute an average residence time for all hyporheic flow paths the residence times for each depth at all four sites were averaged.

Subsurface tracer data from two representative sites is shown in Figure 6. The depth of the hyporheic zone at a particular site was indicated by the depth of penetration of the tracer. In our examples shown in Figure 6 the hyporheic zone was ~10 cm deep at one of the sites (Figure 6a) and 3 cm deep at the other site (Figure 6b). At both sites the stream tracer was detected at the shallowest sampling depth (2.5 cm) just a few minutes following the start of the injection in the stream (Figure 6a and 6b). In contrast, tens of minutes were required for the tracer to reach depths >7 cm at the site with a deeper hyporheic zone. The average hyporheic porewater residence time at all depths at four sites was 17 min, and the range was from 1 to 25 min.

5.1. Flow-Path Scale Determination of the Net Uptake of Manganese in the Hyporheic Zone

After tracer concentrations plateaued in the hyporheic zone and ceased to change with time, porewater samples were removed from each of the six depths (2.5–15 cm) at four sites for complete chemical analysis. In order to determine the rate constant for net chemical uptake of manganese in the hyporheic zone and the percent of removal of manganese by chemical reaction a calculation was needed that accounted for a degree of mixing of surface water and groundwater in the hyporheic zone, the timescale of that mixing, and the net removal of solute by reactive uptake. The following steady state transport equation was used:

$$0 = -\frac{Q}{A}\frac{\partial C_h}{\partial z} + \frac{q_L}{A}(C_L - C_h) - \lambda_h C_h \qquad (7)$$

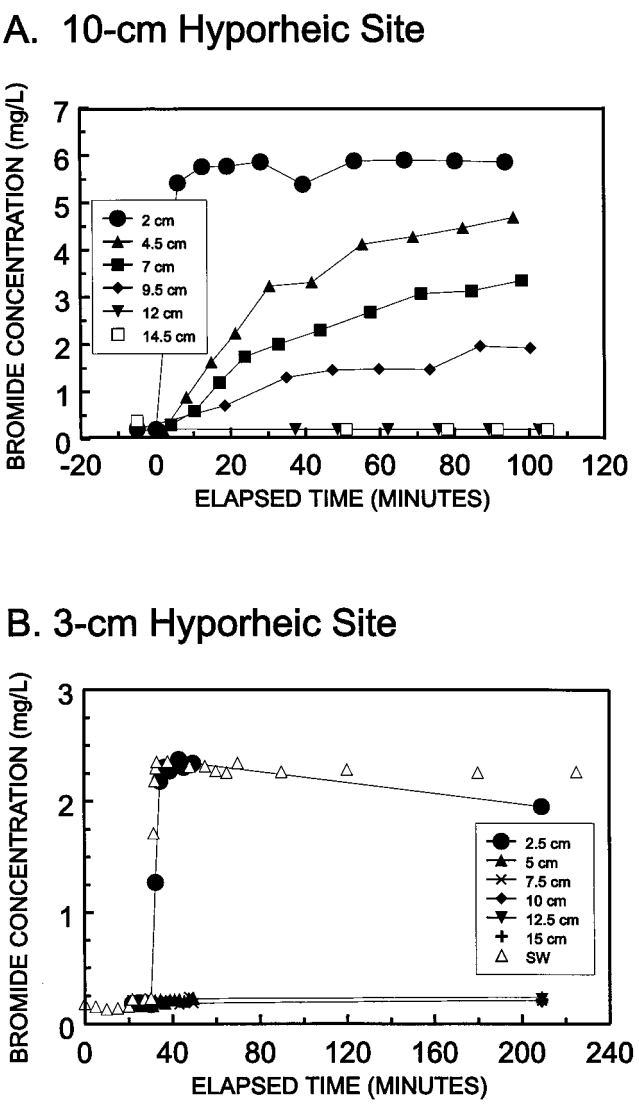

Figure 6. Movement of bromide tracer from stream into hyporheic zone: (a) 10 cm hyporheic site and (b) 3 cm hyporheic site.

where C_h is the concentration of a potentially reactive solute in the hyporheic zone, C_L is the concentration of that solute in groundwater, z is the vertical distance coordinate measured downward from the sediment surface where $z = 0$, q_L is the input of groundwater to the hyporheic zone ($L^3\ L^{-1}\ T^{-1}$), and λ_h is a first-order rate constant describing the net uptake of the solute by chemical reaction in the hyporheic zone (T^{-1}). In order to use (7) to predict solute concentrations at progressively deeper depths in the hyporheic zone we rewrote the equation in finite difference form and rearranged it:

$$\hat{C}_h^{i+1} = C_h^i + \beta^{i+1/2}(C_L - C_h^i) - \lambda_h^{i+1/2}\tau_h^{i+1/2}(C_h^i + C_h^{i+1})/2 \quad (8)$$

The circumflex indicates the target concentration to be calculated; the superscript i refers a particular sample depth; the superscript $i + 1$ refers to the next deepest sampling depth, and the superscript $i + 1/2$ refers to an average value for the interval between sampling depths; $\tau_h^{i+1/2}$ is the travel time of tracer-labeled stream water in a depth increment (calculated as the difference between measured arrival times of stream water tracer depths i and $i + 1$); and $\beta^{i+1/2}$ is the fraction of water contributed from groundwater in a depth increment. The mixing fraction of groundwater, $\beta^{i+1/2}$, was determined from measurements of bromide at each depth after concentrations had plateaued:

$$\beta^{i+1/2} = \frac{Br_h^{i+1} - Br_h^i}{Br_L - Br_h^i} \quad (9)$$

We used (8) to model nonreactive transport of manganese and silica (by setting λ_h equal to zero) at each depth in the hyporheic zone. Figure 7 shows results of modeling nonreactive transport of manganese and silica and compares modeled with measured concentrations. At most depths in the hyporheic zone (indicated by the penetration of bromide) the modeled concentrations for nonreactive transport for manganese were higher (by as much as 20%) compared to measured concentrations. For silica (which we assume was transported without reacting) the model concentrations for nonreactive transport in the hyporheic zone generally matched observations more closely compared to manganese. In groundwater below the hyporheic zone there was little difference between modeled and measured concentrations for either constituent. Our interpretation was that the difference between modeled nonreactive transport and observations estimates the net uptake of dissolved manganese in the hyporheic zone (Figure 7).

We quantified the percent uptake of manganese in the hyporheic zone at each depth interval on the basis of the difference between observed concentrations and modeled concentrations assuming no reaction:

$$f_h^{i+1/2} = \frac{C_h^{i+1} - \hat{C}_h^{i+1}}{\hat{C}_h^{i+1}} 100 \quad (10)$$

Percent uptake of manganese, f_h, was computed for all depths in the sediment reached by the bromide tracer (at the same four sites where porewater residence times were determined; locations are shown by solid circles in Figure 2a). Values of f_h for manganese ranged between 2% and 22% and averaged 9%. Therefore ~9% of the dissolved manganese was removed from stream water and groundwater within a typical depth interval in the hyporheic zone.

How confident are we of the result indicating 9% uptake of dissolved manganese in the hyporheic zone, given that mass balance errors must to some extent affect our calculations? There are two straightforward ways to assess the influence of mass balance errors on our result: (1) first-order uncertainty analysis where analytical uncertainties were propagated in our calculations using standard rules of first-order uncertainty analysis and 2) modeling transport of an additional solute constituent that can be assumed to be nonreactive. For method 1 we used the analytical uncertainties reported in section 3.1 to derive an uncertainty in the percent uptake. For method 2 we assumed the average percent uncertainty for the percent uptake of manganese was estimated by percent uptake that was computed for a conservative constituent, silica. Both methods indicated an average expected mass balance error in f_h of ~±3%. Since the expected uncertainty in f_h is a factor of 3 less than the average value of f_h (9%) computed in this study, we gained confidence that our methods were sensitive enough to reliably estimate the percent uptake of manganese in the hyporheic zone in Pinal Creek basin.

The remaining step in our analysis at the hyporheic-flowpath scale was to compute a net rate of manganese removal in the hyporheic zone, λ_h, by rearranging (8):

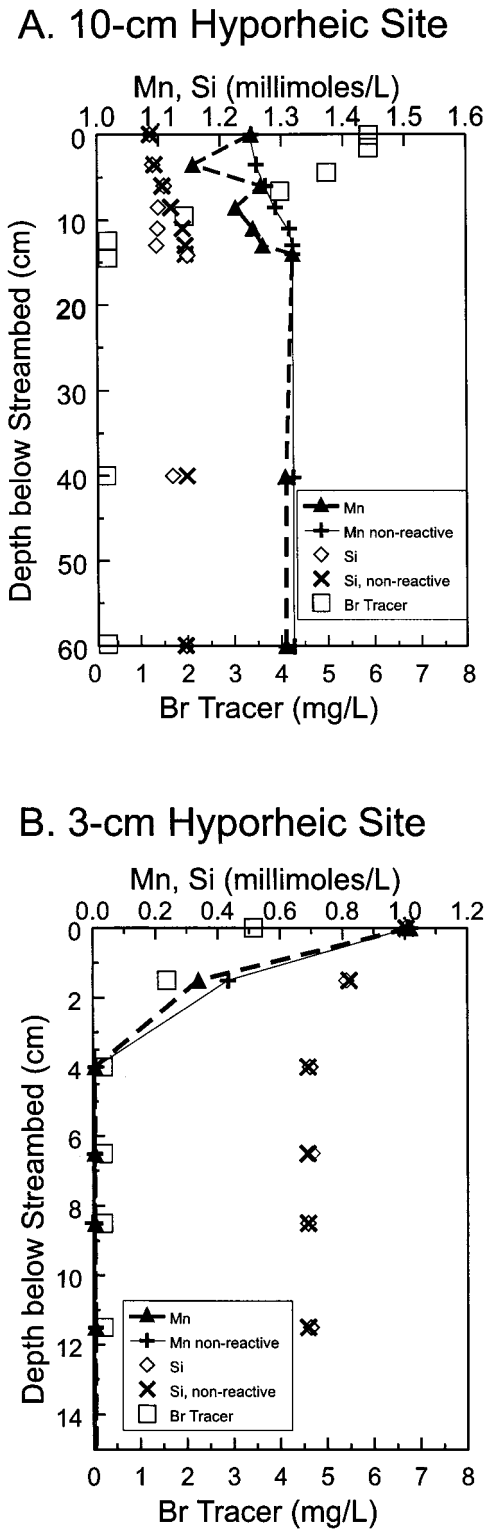

Figure 7. Vertical profiles of dissolved manganese and silica in the hyporheic zone. The presence of the bromide tracer indicates the vertical extent of the hyporheic zone: (a) 10 cm hyporheic site and (b) 3 cm hyporheic site. Nonreactive predictions of manganese and silica concentrations only account for mixing between surface water and groundwater. Differences between nonreactive modeled manganese concentrations and measured manganese concentrations indicate the extent of reactive uptake in the hyporheic zone.

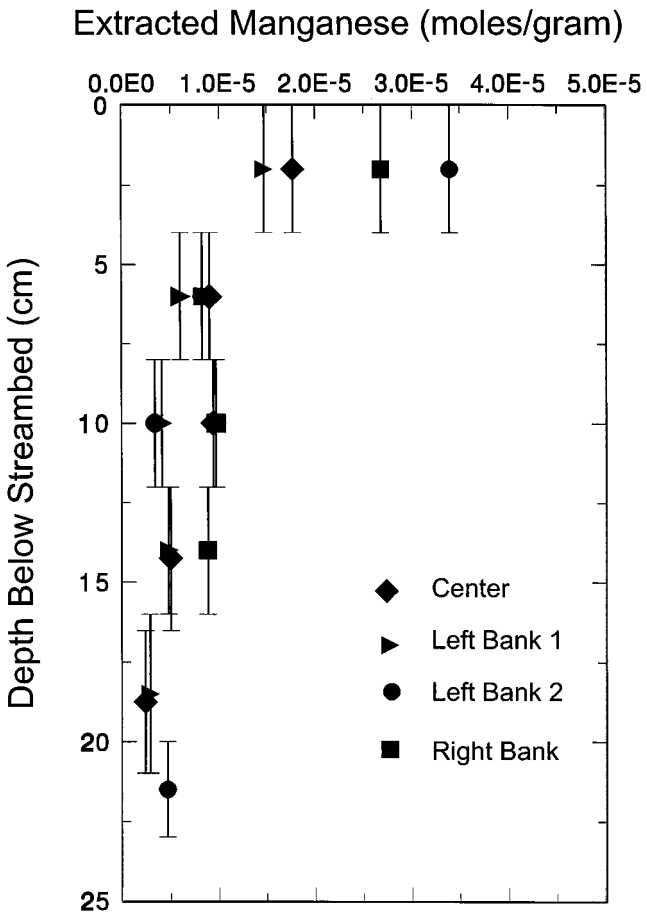

Figure 8. Vertical profile of extracted manganese solid phases from cored sediments in the hyporheic zone. Vertical bars show the length of sediment cores.

$$\lambda_h^{i+1/2} = \frac{C_h^i + \beta^{i+1/2}(C_L - C_h^i) - C_h^{i+1}}{\tau^{i+1/2}(C_h^{i+1} + C_h^i)/2} \tag{11}$$

Rate constants for manganese uptake were computed for all depths reached by the bromide tracer at the same four sites where the percent uptake of manganese, f_h, was determined. The inverse of the rate constant is a time constant for the reaction. Time constants for net manganese uptake ranged from 1 to 12 hours and averaged 2.6 hours.

5.2. Do Sediments Show the Accumulation of Oxidized Manganese Coatings in the Hyporheic Zone?

The concentration of manganese solid phases was greatest near the sediment surface and declined with depth in the hyporheic zone. For example, Figure 8 shows that at a location where the hyporheic zone was thin (~3 cm in depth, as shown in Figures 6b and 7b) the concentration of manganese solid phases in the first depth increment (0–4 cm) was a factor of 4 greater compared to the second increment (4–6 cm) and an order of magnitude greater than the fifth depth increment (16–21 cm). These data support an interpretation that manganese was removed in the hyporheic zone by oxidation and formation of manganese oxyhydroxide phases.

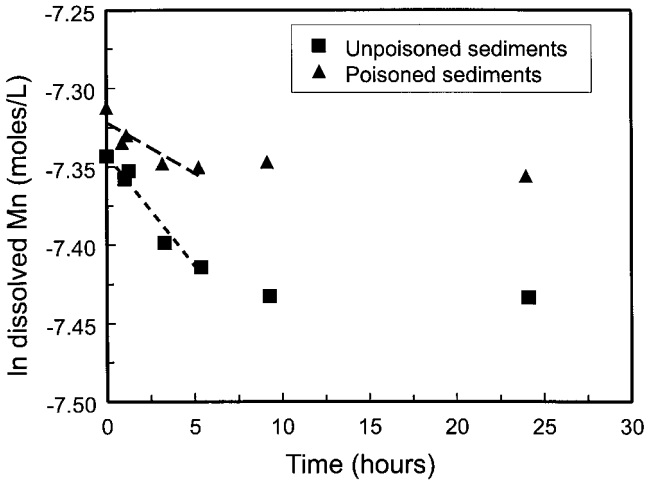

Figure 9. Dissolved manganese uptake in laboratory batch experiments with sediment comparing poisoned and unpoisoned treatments. Dissolved manganese concentrations plotted on *y* axis were corrected by subtracting the reversible component of uptake.

6. Laboratory Scale: Analyses and Results

Dissolved manganese uptake by streambed sediments included an initial rapid component in the first 10 hours followed by a continued uptake at a decreasing rate through 96 hours. Figure 9 shows a typical experimental result; results were only plotted up to 24 hours in order to emphasize the contrast in uptake rates before and after 10 hours. Significantly less uptake in the first 10 hours was observed for poisoned sediments compared to unpoisoned sediments, indicating a large component of microbially enhanced uptake. In contrast, there was little difference in the rate of uptake from 10 to 24 hours in the poisoned and unpoisoned systems (Figure 9). Although the pattern of all results were, in general, similar to Figure 9, the actual amount of uptake appeared to be affected by the amount of preexisting manganese oxide. For example, for a sediment that had a 5 times higher preexisting manganese oxide concentration than the one used in Figure 9, there was both a more rapid initial uptake and a more rapid longer-term uptake for unpoisoned sediments.

The reversible component of manganese uptake determined by isotopic exchange accounted for nearly all the uptake in the initial 0.5 hours. After that, reversible uptake accounted for much less uptake and did not vary significantly for the period between 0.5 and 24 hours. The difference between total uptake and average reversible component measured during the first 24 hours of uptake was therefore used to compute the irreversible component of uptake. The irreversible component of manganese uptake was assumed to characterize oxidation because Mn +3 and +4 oxides are highly insoluble at the *p*H and dissolved oxygen concentration present in the hyporheic zone, which therefore favors oxidation rather than reductive dissolution.

Two distinct linear regions were apparent on semilog plots of manganese concentration (corrected for reversible uptake) versus time, which are treated as two components of irreversible uptake by linearizing separately [*Jannasch et al.*, 1988]. Regressions of the natural log of dissolved manganese versus time from 0–6 hours yielded good fits ($r^2 > 0.9$) (Figure 9). Good fits ($r^2 > 0.9$) also were also obtained for the long-term uptake (10–96 hours). Poorer fits were obtained if the component of reversible uptake was not corrected for.

Apparent rate constants for manganese oxidation were determined by assuming that the irreversible manganese uptake had a first-order dependence on dissolved manganese,

$$\frac{d([\mathrm{Mn}] - [\mathrm{Mn}_x])}{dt} = \lambda([\mathrm{Mn}] - [\mathrm{Mn}_x]) \qquad (12)$$

$$\ln([\mathrm{Mn}] - [\mathrm{Mn}_x])_t = \ln([\mathrm{Mn}] - [\mathrm{Mn}_x])_0 - \lambda t \qquad (13)$$

where [Mn] is the concentration of manganese in solution at time t (in moles L^{-1}), $[Mn_x]$ is the reversible component of Mn^{2+} uptake expressed as an aqueous concentration (in moles L^{-1}), and λ is the first-order rate constant for manganese oxidation (in $time^{-1}$). Only short-term uptake data were used to determine rate constants. We recognize that a log-linear approximation of the oxidation rate assuming a first-order dependence is not appropriate for all situations. For long time periods the rate of manganese oxidation over the entire uptake period is likely better described by a kinetic model that includes additional factors such as the active microbial population, limiting nutrient availability, and availability of reactive sites. However, to obtain laboratory reaction rates to compare with field-derived estimates (for a system with a timescale of stream water transport in Pinal Creek basin of hours and a timescale of hydrologic exchange between surface water and the hyporheic zone of minutes), we felt that the use of a first-order time constant for laboratory Mn uptake fitted to the short-term uptake data (<6 hours) was well justified.

Fitting the short-term uptake data to (13) yielded values of λ of 0.005–0.04 h^{-1}. The apparent first-order rate constants determined in unpoisoned sediments were 2–5 times greater than rate constants determined in poisoned sediments. The lower Mn oxidation rate for poisoned sediments (Figure 9) is consistent with enhancement of Mn oxidation by microbial processes. The linearity of the initial uptake period (<6 hours) suggests that the irreversible uptake (oxidation) on this timescale is well described by a pseudo first-order rate, as has been found in other systems [*Moffett and Ho*, 1996; *Hem*, 1981; *Davies and Morgan*, 1989].

Before comparing laboratory-derived rate constants to field estimates the laboratory rate had to be scaled to actual sediment to water ratios in the hyporheic zone. It was assumed that the rate constant λ is proportional to streambed sediment concentration (grams of dry sediment per liter of stream water), and the reactive sediment fraction (weight fraction of streambed sediment particles <1 mm in diameter). To rescale the rate constant, it was multiplied by the streambed reactive sediment concentration (i.e., the streambed sediment concentration times the reactive sediment fraction) and then divided by the sediment concentration used in laboratory experiments.

A reactive sediment concentration in the streambed of 2520 g L^{-1} was determined from an average streambed porosity of 0.3 and sediment density of 2.7 g cm^{-3} and a reactive sediment fraction of 40%. Our calculation assumed that the reactive sediment fraction (<1 mm diameter) contributes most of the surface area available for manganese oxidation. Considering the fast timescale of laboratory uptake (<6 hours) for all experiments, the range in rescaled rate constants for unpoisoned sediments from Pinal Creek was 0.28–0.69 h^{-1}. The resulting time constants (inverse of rate constants) ranged from 1.5 to 3.6 hours and averaged 2.7 hours.

7. Discussion: Comparisons of Parameters Across Scales—Stream Reach, Hyporheic Flow Path, and Laboratory

7.1. Did the Modeling of Stream-Tracer Injections Characterize Hyporheic Exchange?

Addressing this question was important because of recent work that suggested caution when attempting to characterize the hyporheic zone by modeling stream-tracer experiments [*Harvey et al*., 1996]. At Pinal Creek the agreement between storage-zone dimensions and exchange timescales with direct measurements in the hyporheic zone suggested that the stream-tracer approach did adequately characterize the hyporheic zone (Table 2). The average depth of the storage zone determined by reach-scale modeling (8 cm) agreed relatively well with direct measurements in the hyporheic zone (5 cm). The timescale of hyporheic exchange determined by reach-scale modeling (8 min) was somewhat shorter than estimates derived from subsurface measurements (17 min).

Pinal Creek (with a 1% slope) has a hyporheic zone that is relatively small when compared with steep (5%–10% slope) pool and riffle mountain streams [*Bencala et al*., 1984; *Valett et al*., 1996; *Harvey et al*., 1996]. The ratio of storage to stream cross-sectional areas (A_s/A) at Pinal Creek ranged from 0.03 to 0.38 and averaged 0.16, in comparison with values from mountain streams that often exceed 1. The small extent of the hyporheic zone at Pinal Creek appears to be representative of intermediate gradient streams in the United States that have the coarse sediment needed to conduct subsurface flow (sand, gravel, pebbles, and cobble) but also have a low slope and relatively small roughness features (sand waves, cobbles, and channel bars) which create pressure distributions that can only drive flow through relatively short hyporheic flow paths.

7.2. Comparison of Time Constants for Manganese Uptake Across Scales Using Independent Methods: Stream Reach, Hyporheic Zone, and Laboratory

The next step was to critically evaluate our reach-scale modeling estimates of manganese uptake in hyporheic zones by comparing them with independent estimates made at smaller scales. The time constants were similar for reach-scale modeling, direct measurement in hyporheic flow paths, and laboratory work, averaging 1.3, 2.6, and 2.7 hours, respectively (Table 3). There was extensive overlap in the ranges of time constants determined by reach-scale modeling and laboratory measurements, 1–3 hours and 1–4 hours, respectively, whereas the direct measurements of reaction rates in the hyporheic zone were more variable (1–12 hours). Also, there was a very close agreement between hyporheic-zone field measurements and reach-scale modeling with regard to the fraction of manganese removed from water the hyporheic zone; both estimates were ~9% (Table 3).

Table 2. Comparison Across Scales of Independent Estimates of Hyporheic-Zone Depth d_h and Hyporheic-Zone Porewater Residence Time t_h

Scale	d_h, cm	t_h, min
Basin	8* (4–17)	8† (3–12)
Hyporheic flow path	5‡ (0–15)	17§ (1–25)

Basin-scale values are the averages of reach-scale estimates determined by stream-tracer modeling. Hyporheic-zone values are the averages of estimates determined by subsurface sampling. Ranges in values are given in parentheses.

*The d_h are estimated at the basin scale as the depth of the storage zone in sediments: $d_s = A_s/(\text{wn})$, where A_s is the storage zone cross-sectional area, w is the stream width, and n in sediment porosity.

†The t_h are estimated at the basin scale as the water residence time in the storage zone: $t_s = A_s/(\alpha A)$, where α is the exchange coefficient and A is the stream cross-sectional area.

‡The d_h are estimated at a particular location by observing the depth of penetration of a stream water tracer into the bed.

§The t_s are estimated at a particular location by averaging the travel times for stream water tracer to reach each subsurface sampling point.

Table 3. Comparison Across Scales of Independent Estimates of Dissolved Manganese Uptake

Scale	$1/\lambda_h$, hours	f_h, %
Basin	1.3 (1–3)	8.9 (1–13)
Hyporheic flow path	2.6 (1–12)	9.3 (3–23)
Laboratory	2.7 (2–4)	not applicable

The $1/\lambda_h$ are the time constant for reactive uptake for dissolved manganese in the hyporheic zone, and f_h is the proportion of dissolved manganese taken up by reaction in the hyporheic zone. Sources of data are the same as Table 2, except for laboratory-scale data which came from batch experiments using Pinal Creek sediment. Ranges in values are given in parentheses.

Greater variability in reaction timescales at the hyporheic-flow-path scale (Table 3) probably reflects site to site differences in physical, chemical, and microbiological factors in the hyporheic zone that enhance manganese oxidation. Those factors include physical driving forces for stream water exchange created by roughness features in the stream, the velocity of groundwater inflow which opposes stream water movement into the bed, factors that affect activity levels of Mn-oxidizing bacteria such as pH and oxygen, and the type of surface coating on the sediment and the reactive site density for oxidation of manganese. Determining which factor or combination of factors is the most important in limiting the reaction rate is the subject of ongoing work.

7.3. Basin-Scale Significance of Enhanced Reactions in the Hyporheic Zone

Almost all of the dissolved manganese in Pinal Creek basin is present in a contaminated plume of groundwater that discharges to the perennial stream in its first 2 km. During the initial passage of groundwater discharge through the hyporheic zone and during subsequent exchanges between stream and hyporheic zone a significant proportion of the dissolved manganese is removed by oxidation. Our reach-scale modeling indicated that during the time period of the study (June 1994 and June 1995), ~20% of the dissolved manganese was removed from drainage outflow from Pinal Creek basin by uptake of dissolved manganese in the hyporheic zone.

The significance of this removal can be visualized over the longer term (i.e., the 15 year time period since manganese contamination in groundwater reached Pinal Creek) by modeling long-term transport and comparing results with long-term measurements of streamflow and manganese concentrations that are available from the Pinal Creek Basin Toxic Substances Hydrology Project at USGS in Tucson, Arizona [*Brown et al*., 1997]. In Figure 10 we show the results of extrapolating our modeling information backward in time and comparing modeling results with historic data to show the probable role of the hyporheic zone in removing manganese in

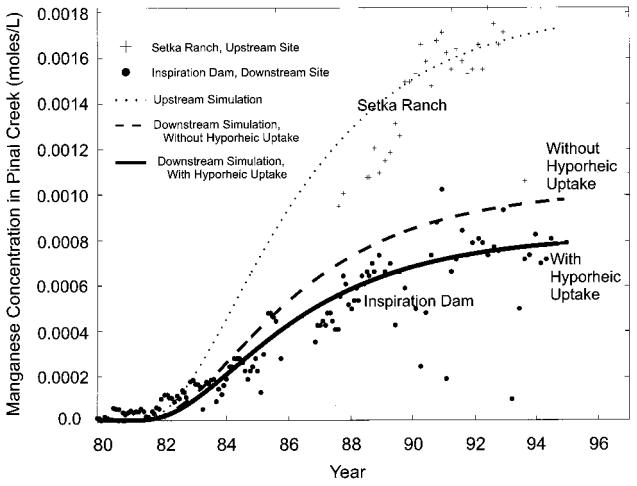

Figure 10. Fifteen year simulation of dissolved manganese transport at Pinal Creek indicating the significance of the hyporheic zone to manganese mass balance at the scale of the drainage basin.

Pinal Creek drainage basin during the 15 years since manganese concentrations began to increase.

The simulation of manganese transport shown in Figure 10 was modeled using the OTIS code [*Runkel and Broshears*, 1991]. Two model reaches were required: one to match the observed concentration history at Setka Ranch and one to simulate transport between Setka Ranch and Inspiration Dam. In reach 1, streamflow, manganese concentration, stream cross-sectional area, and the longitudinal dispersion coefficient were adjusted to approximately match the observed concentration history at Setka Ranch. Parameters in the second reach were set to match the observed streamflow at Inspiration Dam and the resulting groundwater inflow between Setka Ranch and Inspiration Dam. The average concentration of manganese in groundwater inflow in reach 2 was determined from chemistry records available from the USGS [*Brown et al*., 1997]. The remaining parameters in the reach were set equal to average values from our best fit simulations in 1994 and 1995, including the hyporheic-zone cross-sectional area A_s, the stream-hyporheic zone exchange coefficient α, and the manganese reaction rate constant in the hyporheic zone λ_s.

Over the 15 year period of the simulation, there was a relatively good overall match between the long-term trend in simulated and measured manganese concentrations at Inspiration Dam (Figure 10). Observed manganese concentrations at Inspiration Dam were generally more variable than the simulations; this was due in part to episodic storms that cause input from ephemeral tributaries into Pinal Creek that are not represented in our model. The most obvious pattern in both observed and simulated manganese concentrations was that manganese concentrations at Inspiration Dam were considerably lower than at Setka Ranch. That difference reflects two processes: (1) the effect of dilution (apparent as the difference between upstream simulation and downstream simulation without reaction) and (2) the effect of chemical reaction in the hyporheic zone (apparent as the difference between downstream simulations with and without reactive uptake of manganese). Dilution was caused by inflow of groundwater downstream of the point of peak contamination in groundwater (in the vicinity of sampling sites 1 and 2). Dilution decreased (by ~40%) the concentration of dissolved manganese at Inspiration Dam. However, dilution could not decrease the mass flux (or load) of manganese flowing out of the drainage basin. Reactive uptake of manganese in the hyporheic zone, on the other hand, did decrease the load of dissolved manganese flowing out of the drainage basin by ~20%. Overall, the 15 year simulation of manganese transport provided confidence in our conclusion that the hyporheic zone removed a significant proportion of the dissolved manganese that was flowing out of this drainage basin.

7.4. What Are the Limitations of Hyporheic Reactions in Affecting Solute Mass Balances in Drainage Basins?

Our results indicated that 20% of the dissolved manganese that was being transported through Pinal Creek basin was removed by uptake in the hyporheic zone. Our preliminary laboratory uptake experiments suggested that more than half of the removal probably resulted from the enhanced activity of manganese-oxidizing bacteria in the hyporheic zone. The question remains, why was not more manganese removed by uptake in the hyporheic zone at Pinal Creek basin? Is the limitation on removal of manganese more a matter of chemical conditions in the hyporheic zone or physical transport in the stream and hyporheic zone? When evaluated at the largest possible scale, the drainage-basin scale, the significance of hyporheic reactions depends both on the fundamental chemical reactions and on the efficiency of the processing of stream and groundwater flow through hyporheic flow paths. For example, once groundwater has entered the stream, it might be exchanged with the hyporheic zone many times before leaving the drainage basin, each time increasing the opportunity for solute removal by chemical reaction. The amount of turnover of streamflow through the hyporheic zone depends on the velocity in the channel (u) and on the stream-storage-zone exchange coefficient α. Following *Newbold et al*. [1983], we calculated a channel water turnover length L_s for Pinal Creek by dividing the stream velocity u by the stream-storage exchange coefficient α. L_s is the average length in the stream traveled by a solute molecule before it is exchanged with the storage zone; therefore several of these characteristic channel water turnover lengths would be required to divert most or all of the channel water through hyporheic flow paths. L_s was ~1.3 km in Pinal Creek basin. Therefore streamflow would be expected to be entirely exchanged with hyporheic-zone porewater ~2.3 times in the 6 km between Setka Ranch and Inspiration Dam. The hyporheic reaction timescale (~1.3 hours) was somewhat longer than the stream-hyporheic exchange timescale (~10 min), but that was still fast enough that a small but significant proportion of the manganese (~9%) was removed by hyporheic reactions each time stream water passed through the zone. The cumulative effect of exchanging parcels of water several times between stream and hyporheic zone with reaction in the hyporheic zone was to remove ~20% of the load of dissolved manganese before streamflow flowed past Inspiration Dam and out of the drainage basin.

7.5. Cumulative Significance Index for Hyporheic Reactions

Our findings at Pinal Creek can be generalized for other drainage basins and other chemical reactions. We conclude that two conditions are generally going to be needed for hyporheic reactions to be significant at the drainage basin scale. First, timescales of the chemical reaction in the hyporheic zone and turnover of porewater in the hyporheic zone must be

similar (i.e., $1/\lambda_s \approx t_s$), and second, all streamflow must be exchanged with hyporheic porewater once or more within the drainage basin (i.e., $L_s \ll$ the stream length in a drainage basin). Under those conditions, hyporheic reactions are much more likely to affect significantly reactive solute transport and mass balance at the scale of the drainage basin. We suggest a dimensionless significance index for the cumulative effect of hyporheic reactions:

$$R_s = = \frac{\lambda_s t_s L}{L_s} \tag{14}$$

Values of the index and the significance of hyporheic reactions increase either by increasing the time available for reactions (relative to the characteristic reaction time) or by increasing the length of stream available for reactions (relative to the characteristic channel water turnover length). We estimate that ~50% of the reactive constituent is removed at a value of the index of ~2. At Pinal Creek, enhanced manganese oxidation in the hyporheic zone had a significance index of ~0.6. The lower limit of importance will depend on the particular research problem and study site; however, judging from measurement uncertainties at Pinal Creek, we suggest that hyporheic reactions are unlikely to be significant to mass balance in drainage basins where values of R_s are below 0.2.

8. Summary

The results of our study support a conclusion that (1) the rate of manganese oxidation in the hyporheic zone at Pinal Creek basin was significantly enhanced above that in groundwater and in surface water because of the stimulation of microbial activity in the hyporheic zone, (2) the stream-tracer approach was able to accurately quantify the cumulative effect of hyporheic reactions at the scale of an entire drainage basin (verified through comparison of independent estimates of reactive uptake of manganese in the hyporheic zone across four orders of magnitude in spatial scale from centimeters to hundreds of meters), and (3) the cumulative effect of the hyporheic reactions was significant to solute transport and mass balance at the scale of the entire drainage basin because of the similarity of several fundamental timescales and length scales (similarity between hyporheic reaction timescale and hyporheic porewater residence timescale and similarity between the length of stream water turnover through hyporheic flow paths and the stream channel length). When those factors are in balance (the value of the cumulative significance index >0.2), there is likely to be repeated interchange of stream water and subsurface water with ample opportunity for significant reactive uptake before stream water exits a drainage basin. At Pinal Creek, where the cumulative significance index was 0.6, hyporheic reactions removed 20% of the dissolved manganese load exiting the drainage basin.

The agreement between hyporheic transport and reaction parameters obtained by independent approaches at vastly different scales supports our interpretation that enhanced chemical reactions in a small ribbon of sediment surrounding perennial streams can affect solute mass balance at the drainage basin scale. There is much that remains to be determined about the detailed interactions between physical and chemical processes in hyporheic zones. Our preliminary observations suggest that the increase in *p*H and dissolved oxygen in the hyporheic zone due to stream water input are key controls on stimulating microbial enhancement of manganese oxidation, yet much more work is needed. In addition, other work indicates that the fate of trace metal contaminants at Pinal Creek, such as cobalt and nickel, are coupled with the fate of manganese through sorption on manganese oxide coatings that are formed on sediment surfaces in the hyporheic zone. Ongoing work is exploring the greater connection between the fate of manganese and suites of trace metals through interaction in the hyporheic zone.

Acknowledgments. We gratefully acknowledge funding from the USGS Toxic Substances Hydrology Program and from NSF Hydrological Sciences (EAR-9523881). We thank M. Conklin, B. Wagner, J. Brown, D. Gellenbeck, G. Zellweger, D. Graham, S. Ferguson, J. Marble, and H. Flinchbaugh for assistance in fieldwork. For assistance in laboratory analysis, data reduction, and computer simulations we thank Y. Hunter and J. Jackson. We would also like to acknowledge helpful manuscript reviews by USGS colleagues K. Stollenwerk and W. Sanford and reviews for *Water Resources Research* by J. Moore, B. Tebo, and an anonymous reviewer.

References

Bencala, K. E., V. C. Kennedy, G. W. Zellweger, A. P. Jackman, and R. J. Avanzino, Interactions of solutes and streambed sediments, 1, An experimental analysis of cation and anion transport in a mountain stream, *Water Resour. Res*., *20*, 1797, 1984.

Benner, S. G., E. W. Smart, and J. N. Moore, Metal behavior during surface-groundwater interaction, Silver Bow Creek, Montana, *Environ. Sci. Technol*., *29*, 1789, 1995.

Bourg, A. C. M., and C. Bertin, Biogeochemical processes during infiltration of river water into an alluvial aquifer, *Environ. Sci. Technol*., *27*, 661, 1993.

Brown, J. G., R. Brew, and J. W. Harvey, Research on acidic metal contaminants in Pinal Creek basin near Globe, Arizona, *Fact Sheet FS-005-97*, 4 pp., U.S. Geol. Surv., Reston, Va., 1997.

Cerling, T. E., S. J. Morrison, and R. W. Sobcinski, Sediment-water interaction in a small stream: Adsorption of ^{137}Cs by bed load sediments, *Water Resour. Res*., *26*, 1165, 1990.

Chao, T. T., Use of partial dissolution techniques in geochemical exploration, *J. Geochem. Explor*., *20*, 101, 1984.

Davies, S. H. R., and J. J. Morgan, Manganese (II) oxidation kinetics on metal oxide surfaces, *J. Colloid Interface Sci*., *129*, 63, 1989.

Davis, J. A., C. C. Fuller, and A. D. Cook, A model for trace metal sorption processes at the calcite surface: Adsorption of Cd^{2+} and subsequent solid solution formation, *Geochim. Cosmochim Acta*, *51*, 1477, 1987.

Diem, D., and W. Stumm, Is dissolved manganese being oxidized by O_2 in the absence of Mn bacteria or surface catalysts?, *Geochim. Cosmochim. Acta*, *48*, 1571, 1984.

Duff, J. H., F. Murphy, C. C. Fuller, F. J. Triska, J. W. Harvey, and A. P. Jackman, A mini drivepoint sampler for measuring porewater solute concentrations in the hyporheic zone of sand-bottom streams, Limnol. Oceanogr., in press, 1998.

Emerson, S., S. Kalhorn, L. Jacobs, B. K. Tebo, K. H. Nealson, and R. A. Rosson, Environmental oxidation rate of manganese (II): Bacterial catalysis, *Geochim. Cosmochim. Acta*, *46*, 1073, 1982.

Findlay, S., Importance of surface-subsurface exchange in stream ecosystems: The hyporheic zone, *Limnol. Oceanogr*., *40*, 159, 1995.

Findlay, S., D. Strayer, C. Goumbala, and K. Gould, Metabolism of streamwater dissolved organic carbon in the shallow hyporheic zone, *Limnol. Oceanogr*., *38*, 1493, 1993.

Glynn, P., and J. Brown, Reactive transport modeling of acidic metal-contaminated ground water at a site with sparse spatial information, in *Reviews in Mineralogy*, vol. 34, *Reactive Transport in Porous Media: General Principles and Application to Geochemical Processes*, edited by C. I. Steefel, P. Lichtner, and E. Oelkers, pp. 377–438, Mineral. Soc. of Am., Washington, D. C., 1996.

Harvey, J. W., and C. C. Fuller, Association of selected metals with colloidal and suspended particulate material in shallow ground water and surface water at Pinal Creek, Arizona, in *U.S. Geological Survey Toxic Substances Hydrology Program—Proceedings of the Technical Meeting, Colorado Springs, Colorado, September 20–24,*

1993, *Water Resour. Invest. Rep. 94-4014*, U.S. Geol. Surv., Reston, Va., 1996.

Harvey, J. W., B. J. Wagner, and K. E. Bencala, Evaluating the reliability of the stream tracer approach to characterize stream-subsurface water exchange, *Water Resour. Res*., *32*, 2441, 1996.

Heekyung, K., H. F. Hemond, L. R. Krumholz, and B. A. Cohen, In-situ biodegradation of toluene in a contaminated stream, 1, Field studies, *Environ. Sci. Technol*., *29*, 108, 1995.

Hem, J. D., Rates of manganese oxidation in aqueous systems, *Geochim. Cosmochim. Acta*, *45*, 1369, 1981.

Jannasch, H. W., B. D. Honeyman, L. Balistrieri, and J. W. Murray, Kinetics of trace element uptake by marine particles, *Geochim. Cosmochim. Acta*, *52*, 567, 1988.

Kilpatrick, F. A., and E. D. Cobb, Measurement of discharge using tracers, in *Techniques in Water Resources Investigations of the United States Geological Survey*, vol. 3, chap. A-16, pp. 1–52, U.S. Gov. Print. Off., Washington, D. C., 1985.

Kimball, B. A., R. E. Broshears, K. E. Bencala, and D. M. McKnight, Coupling of hydrologic transport and chemical reactions in a stream affected by acid mine drainage, *Environ. Sci. Technol*., *28*, 2065, 1994.

McMahon, P. B., J. A. Tindall, J. A. Collins, K. J. Lull, and J. R. Nuttle, Hydrologic and geochemical effects on oxygen uptake in bottom sediments of an effluent-dominated river, *Water Resour. Res*., *31*, 2561, 1995.

Moffett, J. W., and J. Ho, Oxidation of cobalt and manganese in seawater via a common microbially catalyzed pathway, *Geochim. Cosmochim. Acta*, *60*, 3415, 1996.

Mulholland, P. J., E. R. Marzolf, J. R. Webster, D. R. Hart, and S. P. Hendricks, Evidence that hyporheic zones increase heterotrophic metabolism and phosphorus uptake in forest streams, *Limnol. Oceanogr*., *42*, 443, 1997.

Newbold, J. D., J. W. Elwood, R. V. O'Neill, and A. L. Sheldon, Phosphorus dynamics in a woodland stream ecosystem: A study of nutrient spiralling, *Ecology*, *64*, 1249, 1983.

Payne, T. E., and T. D. Waite, Surface complexation modeling of uranium sorption data obtained by isotopic exchange techniques, *Radiochim. Acta*, *52/53*, 487, 1991.

Runkel, R. L., and R. E. Broshears, One-dimensional transport with inflow and storage (OTIS): A solute transport model for small streams, *Tech. Rep. 91-01*, Cent. for Adv. Decis. Support in Water and Environ. Sci., Univ. of Colo., Boulder, 1991.

Rutherford, J. C., J. D. Boyle, A. H. Elliott, T. V. J. Hatherell, and T. W. Chiu, Modelling benthic oxygen uptake by pumping, *J. Environ. Eng. N. Y.*, *121*, 84, 1995.

Stollenwerk, K. G., Geochemical interactions between constituents in acidic groundwater and alluvium in an aquifer near Globe, Arizona, *Appl. Geochem*., *9*, 353, 1994.

Tarutis, W. J., R. F. Unz, and R. P. Brooks, Behavior of sedimentary Fe and Mn in a natural wetland receiving acidic mine drainage, Pennsylvania, U.S.A., *Appl. Geochem*., *7*, 77, 1992.

Triska, F. J., J. H. Duff, and R. J. Avanzino, The role of water exchange between a stream channel and its hyporheic zone in nitrogen cycling at the terrestrial-aquatic interface, *Hydrobiologia*, *251*, 167, 1993.

Valett, H. M., J. A. Morrice, C. N. Dahm, and M. E. Campana, Parent lithology, surface-groundwater exchange and nitrate retention in headwater streams, *Limnol. Oceanogr*., *41*, 333, 1996.

von Gunten, H. R., and C. Lienert, Decreased metal concentrations in ground water caused by controls of phosphate emissions, *Nature*, *364*, 220, 1993.

Wagner, B. J., and S. M. Gorelick, A statistical methodology for estimating transport parameters: Theory and applications to one-dimensional advective-dispersive systems, *Water Resour. Res*., *22*, 1303, 1986.

Wagner, B. J., and J. W. Harvey, Experimental design for estimating parameters of rate-limited mass transfer: Analysis of stream tracer studies, *Water Resour. Res*., *33*, 1731, 1997.

C. C. Fuller, Water Resources Division, U.S. Geological Survey, 345 Middlefield Road, Mail Stop 465, Menlo Park, CA 94025. (e-mail: ccfuller@usgs.gov)

J. W. Harvey, Water Resources Division, U.S. Geological Survey, 430 National Center, Reston, VA 20192. (e-mail: jwharvey@usgs.gov)

(Received June 18, 1997; revised December 5, 1997;
accepted December 10, 1997.)